

Regional Myocardial Wall Thinning at Multidetector Computed Tomography Correlates to Arrhythmogenic Substrate in Postinfarction Ventricular Tachycardia: Assessment of Structural and Electrical Substrate

Yuki Komatsu, Hubert Cochet, Amir Jadidi, Frédéric Sacher, Ashok Shah, Nicolas Derval, Daniel Scherr, Patrizio Pascale, Laurent Roten, Arnaud Denis, Khaled Ramoul, Shinsuke Miyazaki, Matthew Daly, Matthieu Riffaud, Maxime Sermesant, Jatin Relan, Nicholas Ayache, Steven Kim, Michel Montaudon, François Laurent, Mélèze Hocini, Michel Haïssaguerre and Pierre Jaïs

Circ Arrhythm Electrophysiol. 2013;6:342-350; originally published online March 10, 2013;
doi: 10.1161/CIRCEP.112.000191

Circulation: Arrhythmia and Electrophysiology is published by the American Heart Association, 7272 Greenville Avenue, Dallas, TX 75231

Copyright © 2013 American Heart Association, Inc. All rights reserved.

Print ISSN: 1941-3149. Online ISSN: 1941-3084

The online version of this article, along with updated information and services, is located on the World Wide Web at:

<http://circep.ahajournals.org/content/6/2/342>

Data Supplement (unedited) at:

<http://circep.ahajournals.org/circae/suppl/2013/03/10/CIRCEP.112.000191.DC1.html>

Permissions: Requests for permissions to reproduce figures, tables, or portions of articles originally published in *Circulation: Arrhythmia and Electrophysiology* can be obtained via RightsLink, a service of the Copyright Clearance Center, not the Editorial Office. Once the online version of the published article for which permission is being requested is located, click Request Permissions in the middle column of the Web page under Services. Further information about this process is available in the [Permissions and Rights Question and Answer](#) document.

Reprints: Information about reprints can be found online at:
<http://www.lww.com/reprints>

Subscriptions: Information about subscribing to *Circulation: Arrhythmia and Electrophysiology* is online at:
<http://circep.ahajournals.org/subscriptions/>

Regional Myocardial Wall Thinning at Multidetector Computed Tomography Correlates to Arrhythmogenic Substrate in Postinfarction Ventricular Tachycardia

Assessment of Structural and Electrical Substrate

Yuki Komatsu, MD; Hubert Cochet, MD; Amir Jadidi, MD; Frédéric Sacher, MD; Ashok Shah, MD; Nicolas Derval, MD; Daniel Scherr, MD; Patrizio Pascale, MD; Laurent Roten, MD; Arnaud Denis, MD; Khaled Ramoul, MD; Shinsuke Miyazaki, MD; Matthew Daly, MD; Matthieu Riffaud, MD; Maxime Sermesant, PhD; Jatin Relan, PhD; Nicholas Ayache, PhD; Steven Kim, MEng; Michel Montaudon, MD; François Laurent, MD; Méléze Hocini, MD; Michel Haïssaguerre, MD; Pierre Jaïs, MD

Background—A majority of patients undergoing ablation of ventricular tachycardia have implanted devices precluding substrate imaging with delayed-enhancement MRI. Contrast-enhanced multidetector computed tomography (MDCT) can depict myocardial wall thickness with submillimetric resolution. We evaluated the relationship between regional myocardial wall thinning (WT) imaged by MDCT and arrhythmogenic substrate in postinfarction ventricular tachycardia.

Methods and Results—We studied 13 consecutive postinfarction patients undergoing MDCT before ablation. MDCT data were integrated with high-density 3-dimensional electroanatomic maps acquired during sinus rhythm (endocardium, 509 ± 291 points/map; epicardium, 716 ± 323 points/map). Low-voltage areas (<1.5 mV) and local abnormal ventricular activities (LAVA) during sinus rhythm were assessed with regard to the WT. A significant correlation was found between the areas of WT <5 mm and endocardial low voltage (correlation- $R=0.82$; $P=0.001$), but no such correlation was found in the epicardium. The WT <5 mm area was smaller than the endocardial low-voltage area (54 cm² [Q1–Q3, 46–92] versus 71 cm² [Q1–Q3, 59–124]; $P=0.001$). Among a total of 13 060 electrograms reviewed in the whole study population, 538 LAVA were detected and analyzed. LAVA were located within the WT <5 mm (469/538 [87%]) or at its border (100% within 23 mm). Very late LAVA (>100 ms after QRS complex) were almost exclusively detected within the thinnest area (93% in the WT <3 mm).

Conclusions—Regional myocardial WT correlates to low-voltage regions and distribution of LAVA critical for the generation and maintenance of postinfarction ventricular tachycardia. The integration of MDCT WT with 3-dimensional electroanatomic maps can help focus mapping and ablation on the culprit regions, even when MRI is precluded by the presence of implanted devices. (*Circ Arrhythm Electrophysiol.* 2013;6:342-350.)

Key Words: ablation ■ image integration ■ multidetector computed tomography
■ ventricular arrhythmia ■ ventricular tachycardia

Catheter ablation is an effective therapeutic option in the management of drug-resistant postinfarction ventricular tachycardia (VT).^{1,2} The procedure often relies on substrate-based approaches because of hemodynamic instability, multiple VT morphologies, and noninducibility rendering the VT unmappable.³ Electroanatomic mapping (EAM) is commonly used to identify this substrate, defined as areas of low voltage and local abnormal ventricular activities (LAVA), which are generated by poorly coupled viable fibers within

the scar.⁴⁻⁶ As LAVA are most frequently distributed in the decreased voltage zone, substrate-based approaches largely rely on the delineation of these areas. However, EAM is limited in its ability to detect intramural and nontransmural scars. In addition, suboptimal catheter contact might result in falsely low measurements of normal amplitude resulting in incorrect scar detection.

Clinical Perspective on p 350

Received August 10, 2012; accepted February 19, 2013.

From the Department of Cardiac Electrophysiology, Hôpital Cardiologique du Haut-Lévêque and Université Victor Segalen Bordeaux II, Institut LYRIC, Equipex MUSIC, Bordeaux, France (Y.K., A.J., F.S., A.S., N.D., D.S., P.P., L.R., A.D., K.R., S.M., M.D., M. Hocini, M. Haïssaguerre, P.J.); Department of Cardiovascular Imaging, Hôpital Cardiologique du Haut-Lévêque & Université Victor Segalen Bordeaux II, Bordeaux, France (H.C., M.R., M.M., F.L.); INRIA Sophia Antipolis, Sophia Antipolis, France (M.S., J.R., N.A.); and St. Jude Medical, St. Paul, MN (S.K.).

The online-only Data Supplement is available at <http://circep.ahajournals.org/lookup/suppl/doi:10.1161/CIRCEP.112.000191/-DC1>.

Correspondence to Yuki Komatsu, MD, Hôpital Cardiologique du Haut-Lévêque & Université Victor Segalen Bordeaux II, Institut LYRIC, Equipex MUSIC, Avenue de Magellan, 33604 Bordeaux-Pessac, France. E-mail yk.komat@gmail.com

© 2013 American Heart Association, Inc.

Circ Arrhythm Electrophysiol is available at <http://circep.ahajournals.org>

DOI: 10.1161/CIRCEP.112.000191

Visualization of a potentially arrhythmogenic substrate obtained by cardiac imaging before and during the procedure can help focus mapping and ablation to the culprit regions. Delayed-enhancement MRI may characterize the spatial extent of myocardial scar, including its topography and transmural extent.^{7,8} However, the presence of an implanted cardioverter defibrillator (ICD) is generally considered to preclude the routine use of MRI in the current standard of care and, in any case, degrades the image quality of anterior aspect of the heart. Contrast-enhanced multidetector computed tomography (MDCT) has been shown to provide not only myocardial and vascular anatomy, but also myocardial wall thickness with submillimetric resolution.^{9,10} Myocardial wall thinning (WT) has been reported to correlate with endocardial low voltage,¹¹ but the epicardial voltage and its relationship with LAVA have not been investigated. The objectives of this study were to quantify the relationship between the regional myocardial WT as imaged by MDCT and voltage-defined endo- and epicardial scar, and to assess how regional myocardial WT might predict distribution and characteristics of LAVA.

Methods

Patient Selection

The subjects of this study were 13 consecutive postinfarction patients who underwent iodinated contrast-enhanced MDCT before VT ablation between April 2010 and March 2012. Patients were included if they had episodes of repetitive, sustained VT requiring external cardioversion or ICD interventions. Patients with repetitive premature ventricular contractions or nonsustained VT in the absence of sustained VT were excluded. We also excluded the patients who underwent previous ablation procedures. Written informed consent was obtained from all patients.

Image Acquisition

Contrast-enhanced MDCT was performed on 64-slice CT scanner (SOMATOM Definition, Siemens Medical Solutions, Forchheim, Germany) 1 to 3 days before the ablation procedure. Images were acquired during an expiratory breath-hold with tube current modulation set on end-diastole. CT angiographic images were acquired during the bolus injection of 120 mL of iodinated contrast agent at a rate of 4 mL/s. Acquisition parameters were slice thickness, 0.6 mm; tube voltage, 120 kVp; maximum tube current, 850 mAs; and gantry rotation time, 330 ms.

Image Segmentation

Trans-axial MDCT images comprising the whole heart volume were imported in DICOM format to a local database using the OsiriX3.6.1 software platform (OsiriX Foundation, Geneva, Switzerland). The image processing strategy is illustrated in Figure 1. The epicardium was manually contoured around the left ventricular (LV)-free wall and the right side of the interventricular septum on short axis images. The endocardium and coronary vessels were segmented using automatic region growth segmentation and automatic vessel analysis. Wall thickness segmentations were automatically derived from endo- and epicardial contours. Segmented images were loaded into the CardioviZ3D (INRIA, Sophia Antipolis, France) software package. This software was used to generate 3-dimensional (3D) surface meshes of the endocardium, epicardium, coronary arteries, coronary sinus, and LV myocardial WT from MDCT data. Areas of WT were defined as areas with end-diastole wall thickness of <5 mm and <3 mm, and displayed on both the endo- and epicardial surfaces. We used

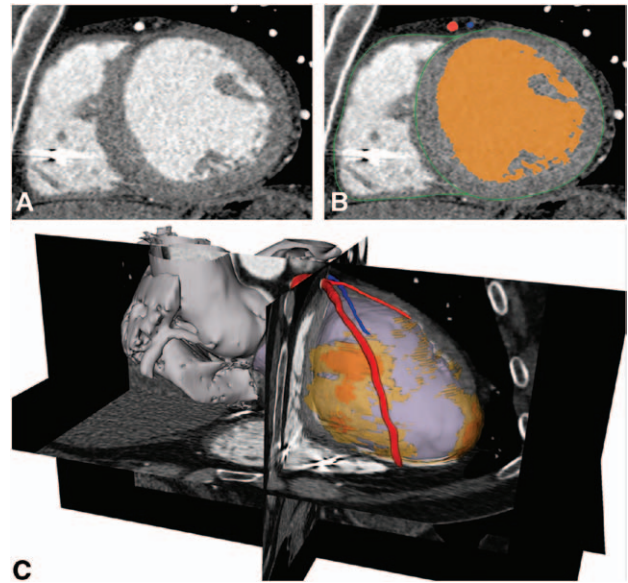


Figure 1. Image processing. Contrast-enhanced multidetector computed tomography images are acquired at end-diastole (A). The endocardium, epicardium, and coronary vessels are segmented (B) and used to compute a 3D anatomic model on which myocardial wall thinning (WT) is mapped using 2 thresholds (orange indicates WT < 3 mm, yellow indicates WT < 5 mm; C).

5-mm value as a cutoff for significant myocardial WT based on a previous report describing the reference values of wall thicknesses by MDCT in a healthy population.¹² These data were imported into 3D-EAM systems and were integrated with the electroanatomic maps.

Electrophysiological Study

A 6-French decapolar catheter (2.5–2 mm, Xtrem, ELA medical, Montrouge, France) was inserted from the right femoral vein and placed into the coronary sinus. The LV endocardium was accessed by transeptal or retrograde transaortic approach. Pericardial access was obtained via a percutaneous subxiphoid puncture.^{6,13} Epicardial mapping was performed if an epicardial substrate was suspected based on VT morphology on a surface ECG, if endocardial mapping did not reveal LAVA, or if VT was induced after complete elimination of endocardial LAVA. EAM during sinus rhythm was performed using CARTO (Biosense Webster, Diamond Bar, CA) in 5 patients or NavX (St. Jude Medical, St. Paul, MN) in 8 patients. Mapping was performed with a 3.5-mm-irrigated tip catheter (NaviStar ThermoCool, Biosense Webster) and/or a multipolar high-density mapping catheter (PentaRay, Biosense Webster). Bipolar signals were filtered from 30 to 250 Hz. We used the following voltage criteria: a peak-to-peak bipolar amplitude of <1.5 mV, defined as the total low-voltage zone; an amplitude of 0.5 to 1.5 mV, the border zone; and an amplitude of <0.5 mV dense scar.³ To assess inducibility, programmed ventricular stimulation was performed at basic drive cycle lengths of 600 and 400 ms with up to triple extra-stimuli decremented down to 200 ms or ventricular refractoriness, whichever occurred first.

Three-Dimensional Registration

For 3D registration of EAM geometry with the MDCT model, identifiable anatomic reference points (coronary sinus, aortic root, LV apex, and mitral annulus [3, 6, 9, and 12 o'clock]) were used as landmarks for alignment and orientation of the EAM and MDCT models. When using Carto, after initial alignment using these fixed reference points as landmarks for registration, automatic surface registration using CartoMerge (Biosense Webster) was performed, as previously described.⁸ When using NavX, a decapolar catheter

was fixed in the coronary sinus, with distal electrodes in the great cardiac vein. Although serving as a stable spatial reference, it also provided a discreet anatomic boundary for guidance of the EAM/MDCT model registration that could be monitored fluoroscopically during the procedure (Figure I in the online-only Data Supplement). The registration algorithm with the NavX Fusion is provided for the dynamic molding of the EAM geometry to the static MDCT surface.¹⁴ After primary registration, the registered model was refined using a second set of fiducial points, judiciously placed in stepwise fashion to further align both surfaces at sites of local mismatch.

Radiofrequency Ablation

When VT was inducible and hemodynamically tolerated, ablation was guided by conventional activation and entrainment mapping.¹ After restoration of sinus rhythm, further ablation targeting LAVA was performed (Figure II in the online-only Data Supplement). In patients with noninducible or poorly tolerated VT, ablation of LAVA was performed during sinus rhythm. As we recently reported,⁶ LAVA due to poorly coupled surviving fibers in the scar was defined as (1) a sharp, high-frequency ventricular potential distinct from the far-field ventricular electrogram, (2) occurring anytime during or most frequently after the far-field ventricular electrogram in sinus rhythm, and (3) sometimes displaying double or multiple components separated by very low-amplitude signals or an isoelectric interval. When LAVA buried in the QRS complex and fused with the far-field ventricular electrogram, various pacing maneuvers were performed to distinguish LAVA from far-field ventricular electrogram.⁶ All areas displaying LAVA were delineated and tagged on the EAM. Irrigated radiofrequency ablation with a power of 25 to 50 W endocardially, and 25 to 35 W epicardially was performed. Where LAVA could be discerned to follow a distinct activation sequence on EAM, the earliest signals were targeted first (Figure II in the online-only Data Supplement).⁶ After ablation, the areas previously displaying LAVA were remapped. In the presence of residual LAVA, radiofrequency ablation was continued. Induction of VT post ablation was repeated with programmed stimulation using the same protocol as preablation induction. The goal and ideal procedural end point was complete elimination of LAVA and noninducibility. In patients with hemodynamically unstable VT, VT inducibility was not systematically retested post ablation.

Data Analysis

The areas of low voltage and WT were manually traced and measured on the EAM system (Figure 2). The overlap between the area with low voltage and the WT <5 mm, the false-negative area (defined as the normal voltage [≥ 1.5 mV] area lying within the WT area), and the false-positive area (defined as low voltage [< 1.5 mV] area lying outside the WT area) were measured and expressed in respective percentages. Whether the region of LAVA was inside or outside of the WT <5 mm and the WT <3 mm was assessed, and, when outside, its distance from the border of the WT area was measured. The analysis of LAVA characteristics included (1) the electrogram amplitude, (2) the duration from the onset to the end of LAVA, and (3) the interval from the end of the QRS complex on surface ECG to the end of LAVA to estimate the degree of local conduction delay.

Statistical Analysis

Categorical data were expressed as numbers and percentages. Continuous data for normally distributed variables were expressed as mean \pm SD and were compared using Student paired *t* test. The WT and low-voltage area were expressed as median (25th, 75th percentiles) and were compared using Wilcoxon signed-rank test because these data were skewed. For assessing the correlation between the WT and low-voltage area, Spearman rank correlation coefficients were calculated. As the data of electrogram characteristics were also non-normally distributed variables, they were presented as median

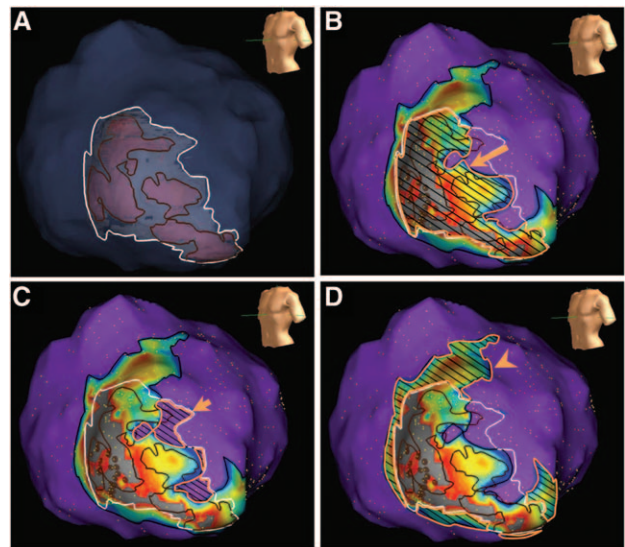


Figure 2. Comparison the wall thinning (WT) and low voltage and local abnormal ventricular activities (LAVA) localization on the 3D electroanatomic mapping (EAM) system. The WT that is extracted from multidetector computed tomography is superimposed on the EAM geometry (epicardium), and areas of WT <5 mm (white line) and <3 mm (brown line) are manually traced and measured (A). The WT <5 mm can be compared with low-voltage area. The area of overlap (B, long arrow), false-negative (C, short arrow), and false-positive (D, arrow head) are measured. The regions of LAVA are tagged, and whether the regions of LAVA are inside or outside of the WT <5 mm and WT <3 mm can be assessed.

and quartiles and were compared using Friedman test. All the tests were 2-tailed, and a *P* value of <0.05 was considered statistically significant.

Results

Thirteen patients (12 men; 61 \pm 12 years) were studied. Patient characteristics are summarized in Table 1. Detailed LV mapping was performed endocardially in all and epicardially in 9 patients. Mean number of mapping points was 509 \pm 291 and 716 \pm 323 points/map on the endo- and epicardium, respectively. The average of mapping density was 4.8 \pm 2.7 points/cm² and 3.5 \pm 2.6 points/cm² on the endo- and epicardium, respectively. The electric infarcts (bipolar voltage <1.5 mV) were located anteriorly in 7 (54%), inferiorly in 2 (15%), and laterally in 4 (31%) patients. No significant difference was seen in the mapping density between the low-voltage and normal voltage area (4.3 \pm 3.1 points/cm² versus 3.7 \pm 2.1 points/cm²; *P*=0.13).

Low-Voltage Area and WT

Regional myocardial WT <5 mm and <3 mm could be identified, and the integration of segmented WT with 3D-EAM systems was feasible in all patients. Figure 3 shows a typical combined endo- and epicardial map. The localization of regional WT corresponded to voltage-defined scar. The area of WT and voltage-defined scar in each patient is shown in Table 2. In patients who underwent both the endo- and epicardial mapping, a significant correlation was found between the WT <5 mm and low-voltage area (<1.5 mV) on the endocardium

Table 1. Patient Characteristics

Pt No.	Age, y	Sex	LVEF, %	ICD	Antiarrhythmic Drug Before Procedure	No. of Prior Procedures	No. of Induced VTs	Map
1	64	W	37	Yes	Amiodarone+β-blocker	0	2	Epi and Endo
2	31	M	38	No	Amiodarone+β-blocker	0	4	Endo
3	62	M	20	No	Amiodarone+β-blocker	0	5	Endo
4	73	M	27	Yes	Amiodarone+β-blocker	0	3	Epi and Endo
5	54	M	15	Yes	Amiodarone+β-blocker	0	3	Epi and Endo
6	65	M	40	Yes	Sotalol+β-blocker	0	0	Endo
7	73	M	30	No	Amiodarone+β-blocker	0	2	Epi and Endo
8	68	M	20	Yes	Amiodarone+β-blocker	0	2	Epi and Endo
9	65	M	25	Yes	Amiodarone+β-blocker	0	0	Epi and Endo
10	57	M	30	Yes	Sotalol+β-blocker	0	1	Epi and Endo
11	72	M	23	Yes	β-blocker	0	1	Epi and Endo
12	45	M	30	Yes	Amiodarone+β-blocker	0	0	Epi and Endo
13	66	M	15	Yes	Amiodarone+β-blocker	0	5	Endo

Endo indicates endocardium; Epi, epicardium; ICD, implantable cardioverter defibrillator; LVEF, left ventricular ejection fraction; M, men; VT, ventricular tachycardia; and W, women.

(correlation- $R=0.82$; $P=0.001$). However, the area of WT <5 mm measured on the endocardium was significantly smaller than the low-voltage area (54 [46–92] cm² versus 71 [59–124] cm²; $P=0.001$). On the epicardium, there was no significant correlation between the WT (45 [42–61] cm²) and low-voltage area (52 [51–68] cm²; correlation- $R=0.55$; $P=0.13$). As shown in Figure 4, the mean percentage of false-negative area was smaller on the endocardium compared with the epicardium (4±3% versus 14±7%; $P=0.001$). For the false-positive area, there was no such difference (23±8% versus 23±7%; $P=0.94$). The overlap between the area with low-voltage and the WT <5 mm was greater on the endocardium than on the epicardium (73±8% versus 62±3%; $P=0.004$).

Distribution and Characteristics of LAVA

Among a total of 13 060 electrograms reviewed in the whole study population, we detected and analyzed 538 electrograms

displaying LAVA (endocardium, 370; epicardium, 168). The distribution of LAVA in dense scar, border zone, and normal voltage was 74%, 23%, and 3%, respectively. LAVA with normal voltage were not farther than 19 mm from the border of the low-voltage area. Most of the LAVA (469/538 [87%]) were located within the WT <5 mm, and 242 of 538 (45%) were detected within the thinnest area (WT<3 mm). Although 13% of LAVA were located outside the WT <5 mm, they were not farther than 23 mm from its border. On the endocardium, LAVA were mainly located in the 3 mm<WT<5 mm (WT<3 mm, 37%; 3 mm<WT<5 mm, 49%; outside, 14%). In contrast, on the epicardium, more than half of LAVA were located within the WT<3 mm (WT<3 mm, 59%; 3 mm<WT<5 mm, 33%; outside, 8%). The density of LAVA in the low-voltage area was significantly lower than that in the 3 mm<WT<5 mm on the endocardium (0.35±0.21 versus 0.50±0.37 points/cm²; $P=0.043$; Figure 5A) and that in the WT <3 mm on the

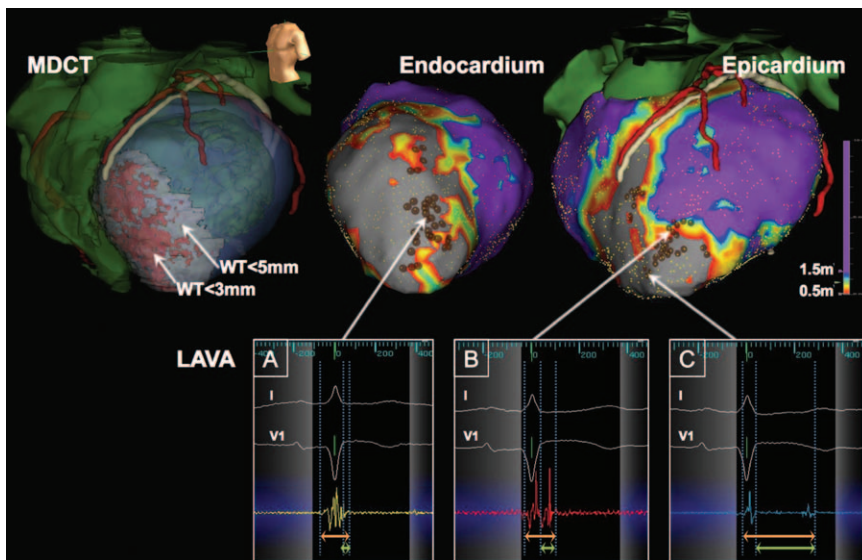


Figure 3. Endo- and epicardial voltage maps and local abnormal ventricular activities (LAVA). The location of wall thinning (WT) corresponds to the low voltage. On the endocardium, the low-voltage area was larger than the WT area. Epicardial fat along the coronary vessels results in false-positive area. Most of the LAVA were located within the WT<5 mm. The analysis of LAVA characteristics included (1) the electrogram amplitude, (2) electrogram duration (orange arrow), and (3) delay after the QRS-end (green arrow). On the endocardium, LAVA within the 3 mm<WT<5 mm (A) exhibit sharp and high-frequency signals with relatively short electrogram duration and short delay after QRS-end. On the epicardium, LAVA within the 3 mm<WT<5 mm (B) represent relatively larger amplitude and longer delay after QRS-end than LAVA (A). LAVA within the WT <3 mm on the epicardium (C) have low amplitude and very late component after QRS. MDCT indicates multidetector computed tomography.

Table 2. Area of WT and Low-Voltage Area

Pt No.	Location	Endocardium		Epicardium		
		WT Area (<3 mm/<5 mm)	Low-Voltage Area (<1.5 mV)	Location	WT Area (<3 mm/<5 mm)	Low-Voltage Area (<1.5 mV)
1	Anteroseptal	29/48	59	Anterior	27/45	52
2	Inferior	8/37	40
3	Posterolateral	11/48	54
4	Anteroseptal	13/61	71	Anterior	10/42	51
5	Anteroseptal	78/120	154	Anterior	70/102	141
6	Posterolateral	75/92	126
7	Anteroseptal	14/42	60	Anterior	13/40	40
8	Posterolateral	67/96	124	Posterolateral	67/96	98
9	Anterior	29/45	62	Anterior	29/45	45
10	Posterolateral	24/54	76	Posterolateral	24/54	68
11	Inferoseptal	17/54	58	Inferior	12/40	53
12	Anteroseptal	76/110	120	Anterior	35/61	51
13	Anteroseptal	59/88	145
Median (quartiles)		29 (14–67)/54 (46–92)*	71 (59–124)*		23 (13–35)/45 (42–61)	52 (51–68)

Data are presented as cm². WT indicates wall thinning.

* $P < 0.05$ (WT < 5 mm area vs low-voltage area on the endocardium).

epicardium (0.29 ± 0.18 versus 0.44 ± 0.29 points/cm²; $P = 0.038$; Figure 5A).

As shown in Table 3, we observed significant differences in the characteristics of LAVA (electrogram duration, delay after the QRS-end, and electrogram amplitude) among the regions in the WT < 3 mm, 3 mm < WT < 5 mm, and outside the WT. Of note, very late LAVA (delay from QRS-end > 100 ms) were almost exclusively detected within the WT < 3 mm (93%), and their amplitudes were < 0.5 mV (Figure 5B). In contrast,

LAVA with amplitude > 0.5 mV were not very late, and most of them were located within the 3 mm < WT < 5 mm or outside the WT area (Figure 5B).

Radiofrequency Ablation

The integration of WT segmentation with 3D-EAM allowed the operator to concentrate on the areas displaying most of the LAVA. Radiofrequency ablation targeting LAVA was performed endocardially first in all patients and was required epicardially in 9 patients. In total, 28 VTs (induced or spontaneous) were observed in 10 patients, and 15 of 28 (54%) were hemodynamically unstable. Thirteen hemodynamically stable VTs induced by programmed stimulation were mapped in 7 patients using conventional and entrainment mapping. The sites where the ablation successfully terminated VT were on the endocardium in 10 and on the epicardium in 3. Of these, 4 of the endocardial and 2 of the epicardial sites were located within the WT < 5 mm (Figure III in the online-only Data Supplement). Although ablation terminated the remaining 7 VTs outside the WT < 5 mm, the ablation sites were not > 7 mm away from the border of WT < 5 mm area. After termination of VT in these cases, further ablation targeting LAVA was performed during sinus rhythm. The substrate information provided by the WT was also useful for remapping after ablation of LAVA, not to miss the residual delayed potentials within the thinnest area. Complete elimination of LAVA was achieved in 11 of 13 patients. During a follow-up of 10 ± 8 months, ICD interrogation showed an episode of recurrent VT in 2 patients. One patient required ICD shock, and the other required antitachycardia pacing to terminate the recurrent VT.

Discussion

This study demonstrates the relationship between the regional myocardial WT and arrhythmogenic substrate in postinfarction VT. The novel findings are that (1) despite a good correlation between the area of regional WT < 5 mm and endocardial

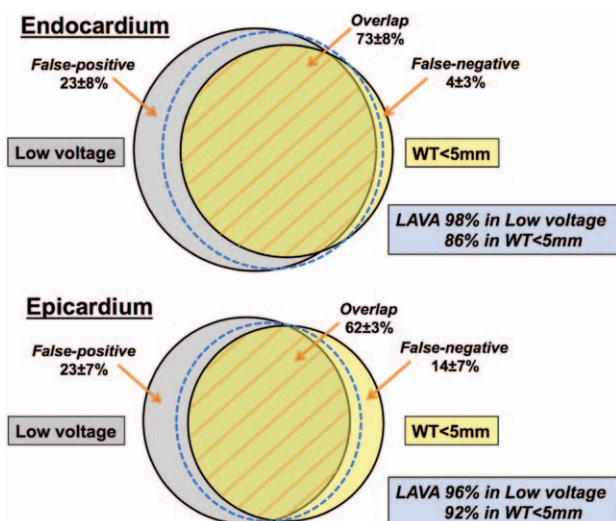


Figure 4. The regional wall thinning (WT) area vs low-voltage area. Low voltage is considered as the gold standard and the WT is analyzed accordingly. The false-negative area was smaller on the endocardium than the epicardium ($4 \pm 3\%$ vs $14 \pm 7\%$; $P = 0.001$). For the false-positive area, there was no such difference ($23 \pm 8\%$ vs $23 \pm 7\%$; $P = 0.94$). The overlap area was greater on the endocardium than on the epicardium ($73 \pm 8\%$ vs $62 \pm 3\%$; $P = 0.004$). The blue dotted line shows local abnormal ventricular activities (LAVA) distribution. Endocardial LAVA were detected in low-voltage area (98%) and in WT (86%), and epicardial LAVA in low-voltage area (96%) and in WT (92%).

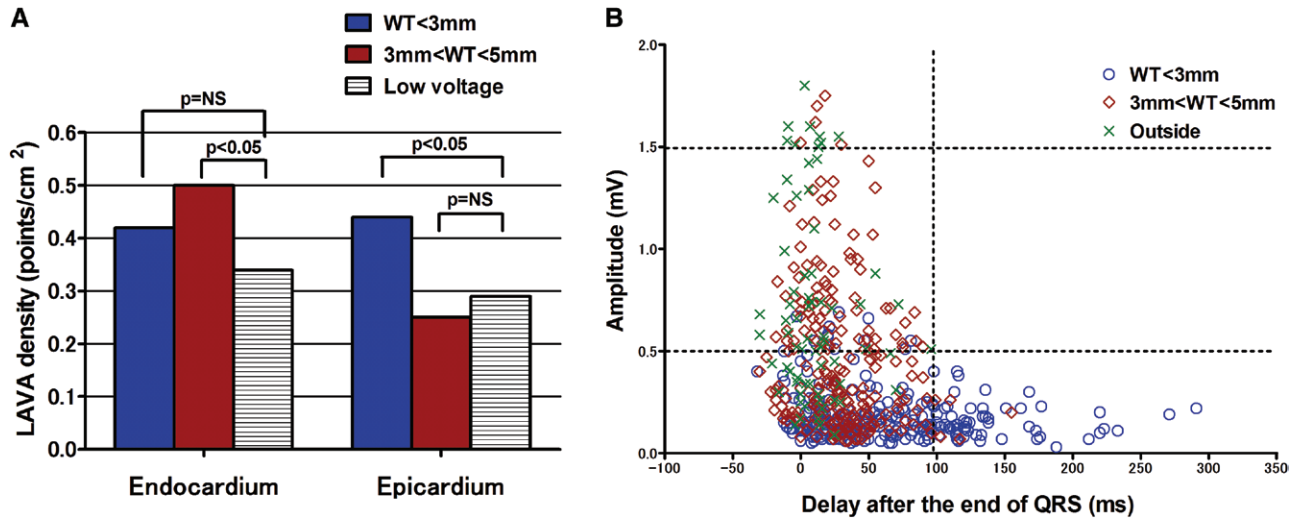


Figure 5. Distribution and characteristics of local abnormal ventricular activities (LAVA). The LAVA density in the low-voltage area was lower than that in the 3 mm < wall thinning < 5 mm on the endocardium ($P=0.043$) and in the WT < 3 mm on the epicardium ($P=0.038$; **A**). Scattered plot of all LAVA points grouped by the wall thickness is shown in **B**. Very late LAVA (delay from the QRS-end > 100 ms) are exclusively detected within the WT < 3 mm. Their amplitudes were < 0.5 mV. In contrast, LAVA with amplitude > 0.5 mV were not very late, and most of them were located within the 3 mm < WT < 5 mm or outside the WT.

voltage-defined scar, WT area is substantially smaller than the low-voltage area; (2) 87% of LAVA are located within the WT < 5 mm, and the remaining 13% are not farther than 23 mm from its border; and (3) the vast majority of very late LAVA are present within the thinnest region (93% in the WT < 3 mm). The present methodology using MDCT provides important information for identification and characterization of arrhythmogenic substrate in postinfarction VT and can help focus mapping and ablation on the culprit regions even when potential substrate imaging by MRI is precluded by the presence of implanted devices.

Regional Myocardial WT and Low-Voltage Area

Myocardial WT is frequently observed in areas of previous myocardial infarction, as a result of cellular loss according to interstitial remodeling in ischemic cardiomyopathy.¹⁵

As expected, we found a significant correlation between the area of endocardial voltage-derived scar and regional WT. This finding is in accordance with a previous report, which has described that MDCT-derived data, including the LV wall thickness, correlate with abnormal voltage locations.¹¹ However, despite a good correlation, WT < 5 mm was consistently smaller than endocardial low-voltage area. This is likely to be because of the 5-mm threshold used in this study. Nontransmural heterogeneous scars and border zone may not contribute to the WT, resulting in MDCT's reduced sensitivity in endocardial scar depiction. This underestimation of the real substrate which may be even more pronounced as voltage mapping is known to miss nontransmural and heterogeneous scars, which could be demonstrated as delayed enhancement on MRI or hypoperfusion on MDCT. The WT allows us to depict most of the scar, but one should keep in mind that mapping should

Table 3. Characteristics of LAVA in Relation to the Wall Thickness

	WT < 3 mm	3 mm < WT < 5 mm	Out of the WT
Electrogram duration, ms			
Endocardium	152 (123 to 194)	125 (101 to 150)	102 (90 to 117)
Epicardium	150 (119 to 202)	121 (97 to 144)	94 (80 to 113)
Total	151 (122 to 194)	123 (100 to 148)	102 (90 to 115)
Delay after QRS-end, ms			
Endocardium	47.5 (18.0 to 95.3)	27.0 (9.8 to 45.3)	6.0 (-5.8 to 15.3)
Epicardium	48.5 (18.0 to 94.8)	22.0 (12.0 to 50.0)	8.0 (1.0 to 23.0)
Total	48.0 (18.0 to 95.3)	25.0 (11.0 to 46.0)	6.0 (-3.5 to 15.5)
Amplitude of LAVA, mV			
Endocardium	0.13 (0.09 to 0.22)	0.27 (0.16 to 0.54)	0.57 (0.33 to 1.02)
Epicardium	0.15 (0.12 to 0.21)	0.56 (0.33 to 0.83)	0.71 (0.43 to 0.88)
Total	0.14 (0.10 to 0.21)	0.32 (0.18 to 0.61)	0.57 (0.34 to 0.94)

Data are presented as median (25th to 75th percentiles). $P < 0.05$ for all line. LAVA indicates local abnormal ventricular activities; and WT, wall thinning.

be extended to ≈ 20 mm from its border not to miss LAVA and critical areas for VT termination.

Less false-negative and greater overlap percentage between the WT and voltage-defined scar were found on the endocardium compared with the epicardium. Although previous studies have reported the substantial correlation between endocardial low voltage and scar as depicted by cardiac imaging,^{7,8,11} this is the first to systematically compare the epicardial low voltage with scar at cardiac imaging in patients with postinfarction VT. The better endocardial match observed may be a consequence of the fact that the ischemic scar usually progresses from the subendocardium to the epicardium within the territory of the culprit coronary artery. In addition, more collateral arteries will limit the epicardial scar. Therefore, except for transmural scar, a lower impact of infarct-related scar on epicardial voltage is to be expected. This might explain the larger percentage of normal voltage area lying within the WT on the epicardium compared with the endocardium. Besides, the overlying epicardial fat¹⁶ may contribute to the decreased voltage area lying outside the WT, especially in the right ventricular epicardium where the WT was not mapped. Nevertheless, it is noteworthy that the localization of regional WT corresponds to epicardial low voltage with 62% overlap, implying that the WT data can provide complementary information for identification of the genuine abnormal voltage on the epicardium.

Distribution and Characteristics of LAVA With Regard to the WT

This study is the first to assess the relationship between the myocardial regional WT and the distribution and characteristics of LAVA. The regional WT was associated with the areas where LAVA were recorded. In particular, all LAVA were located within 23 mm from the border of WT <5 mm. When comparing the LAVA distribution with low-voltage area, normal voltage LAVA were only 3% and were not farther than 19 mm from the border of low-voltage area. However, the low-voltage area may not be highly specific in prediction of LAVA distribution. We found that LAVA were mainly located in the 3 mm < WT < 5 mm on the endocardium and within the WT < 3 mm on the epicardium. The LAVA densities in those areas were significantly higher than in the low-voltage area. These findings suggest that the integration of the WT data with 3D-EAM system can allow the operator to concentrate on more specific areas where LAVA were more likely to be found. Because complete elimination of LAVA is associated with a better prognosis,⁶ the present methodology has the potential to play an important role in guiding substrate-based ablation targeting their complete elimination.

It is of special interest that there are significant differences in the characteristics of LAVA with regard to the myocardial wall thickness. Very late LAVA were exclusively detected within the thinnest regions. Although the scar depth cannot be estimated with the present methods, our findings are in line with the previous studies describing that the most delayed signals are usually detected deep inside the dense scar rather than at the scar border zone.^{17,18} Previous studies have demonstrated that very late abnormal signals can improve the specificity of prediction of critical isthmus of VT.^{18,19} Hence, the propensity

of very delayed LAVA to be distributed within the thinnest regions can be useful to predict the areas which are critical to the reentrant VT circuit. Nonetheless, the latest LAVA may not be targeted first. When a definite sequence of activation of LAVA is clearly discerned, ablation of earliest LAVA in the peri-infarct region can eliminate the later LAVA within the dense scar. The conducting channels of the VT reentrant circuit are considered to have the interconnecting pathways with orthodromic activation from the edge to the inner of the scar.²⁰

A prior study demonstrated that successful ablation sites of postinfarction VT may be located in the peri-infarct area with tissue heterogeneity assessed by contrast-enhanced MRI.²¹ Another study described that successful ablation was achieved at the border zone in 68% and at the dense scar in 18%. They did not attempt to ablate at VT exit sites in the first instance, so the proportion of successful ablations at the exit site in the scar border zone was not overestimated.²² In our study, approximately half of the successful ablation sites where the ablation terminated VT were located outside the WT area, albeit very adjacent to its border. These findings suggest that the sites where the ablation terminates VT are likely to be located in the peri-infarct area, possibly corresponding to the nontransmural and heterogeneous scar border zone, which can escape detection as severe WT. This is supported by the findings of a previous study wherein WT at the infarct border zone and gradient of local wall thickness could predict the location of critical isthmuses in a model of VT reentry.²³

Study Limitations

This study was performed using 2 EAM systems that differ in terms of registration methods. The possibility of misregistration of the cardiac imaging with the 3D-EAM systems cannot be excluded. In the present study, the cross-platform design was chosen to confirm the consistency of the findings on the 2 most widely used EAM platforms. Our results confirm that the integration of regional myocardial WT with both 3D-EAM systems is feasible using Cardioviz3D allowing to display high-quality segmentation of multiple 3D-reconstructed objects. However, there might be possible differences in LAVA characteristics, such as amplitude, due to the differences in mapping electrodes. Although there has been no case in our experience where LAVA would have been identified at 1 site with 1 catheter but not with the other one, multipolar mapping catheter with a smaller diameter and shorter inter-electrode spacing than 4-mm tip mapping catheter might be more sensitive to detect small and complex potentials. In this study, we had 5 patients mapped without multipolar mapping catheter for technical reasons of Carto system's compatibility. If multipolar mapping catheter had been available in these patients, more numbers of LAVA might have been detected in higher density electroanatomic maps.

Although our results were consistent among patients, small study population might be biased toward the patients with discrete scars. Small severe WT may be less likely to be identified in patients with relatively small infarct regions, which might be characterized as nontransmural scars. Our results need to be explored further with larger population especially including the patients in whom scar might be more heterogeneous and geometrically more complex. Delayed-enhancement MRI

would have been helpful to compare the regional WT with spatial localization and transmuralty of scar.

There is a potential bias in the results of LAVA distribution because the operator was not blinded to the location of the WT during the mapping procedure. However, the mapping density was not significantly different between the regions with and without containing LAVA. This result implies that the pre-procedural information of the WT location had no significant impact on the mapping strategy.

Lastly, ICD-related artifacts are sometimes observed at the apex, and this might have induced some errors in the measurement of wall thickness. However, these artifacts are of limited extent on the LV wall, essentially located in the septo-apical segment, as opposed to the right ventricular wall. In this study, no obvious effect was noted on quantifying the LV apical wall thickness.

Conclusions

The integration of regional myocardial WT imaged by multidetector CT with 3D EAM systems is feasible and can be used to guide substrate-based ablation in postinfarction VT. The region of and around myocardial WT harbor all LAVA sites, of which elimination is related to a favorable clinical outcome. The thinnest areas are associated with the latest electric activities demonstrating a structure–function relationship.

Sources of Funding

This research was supported in part by Leducq Foundation grant number 09 CVD 03.

Disclosures

None.

References

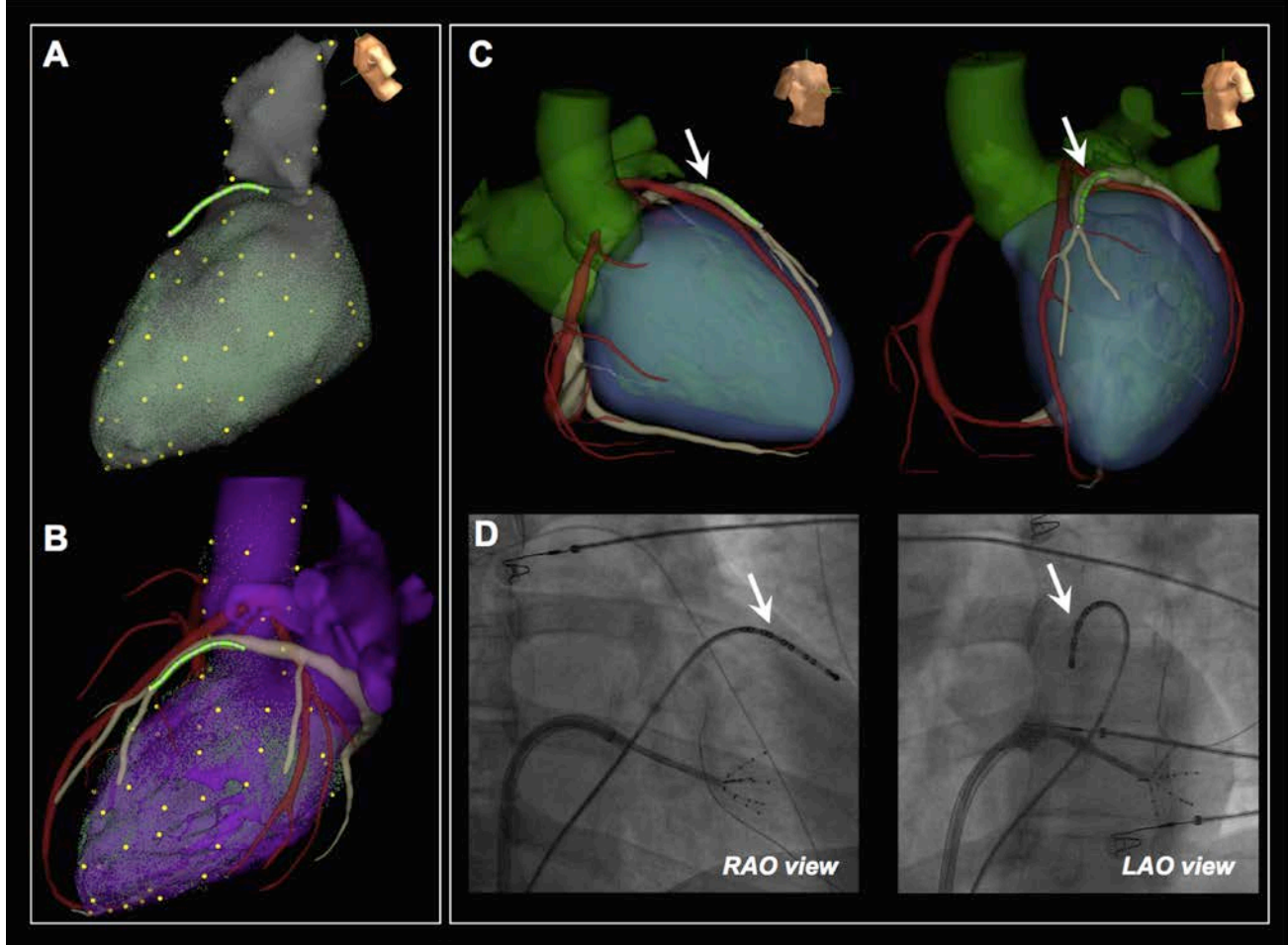
- Stevenson WG, Khan H, Sager P, Saxon LA, Middlekauff HR, Natterson PD, Wiener I. Identification of reentry circuit sites during catheter mapping and radiofrequency ablation of ventricular tachycardia late after myocardial infarction. *Circulation*. 1993;88(4 pt 1):1647–1670.
- Reddy VY, Reynolds MR, Neuzil P, Richardson AW, Taborsky M, Jongnarangsin K, Kralovec S, Sediva L, Ruskin JN, Josephson ME. Prophylactic catheter ablation for the prevention of defibrillator therapy. *N Engl J Med*. 2007;357:2657–2665.
- Marchlinski FE, Callans DJ, Gottlieb CD, Zado E. Linear ablation lesions for control of unmappable ventricular tachycardia in patients with ischemic and nonischemic cardiomyopathy. *Circulation*. 2000;101:1288–1296.
- Gardner PI, Ursell PC, Fenoglio JJ Jr, Wit AL. Electrophysiologic and anatomic basis for fractionated electrograms recorded from healed myocardial infarcts. *Circulation*. 1985;72:596–611.
- de Bakker JM, van Capelle FJ, Janse MJ, Tasseron S, Vermeulen JT, de Jonge N, Lahpor JR. Slow conduction in the infarcted human heart. ‘Zigzag’ course of activation. *Circulation*. 1993;88:915–926.
- Jais P, Maury P, Khairy P, Sacher F, Nault I, Komatsu Y, Hocini M, Forelax A, Jadidi AS, Weerasoorya R, Shah A, Derval N, Cochet H, Knecht S, Miyazaki S, Linton N, Rivard L, Wright M, Wilton SB, Scherr D, Pascale P, Roten L, Pederson M, Bordachar P, Laurent F, Kim SJ, Ritter P, Clementy J, Haïssaguerre M. Elimination of local abnormal ventricular activities: a new end point for substrate modification in patients with scar-related ventricular tachycardia. *Circulation*. 2012;125:2184–2196.
- Desjardins B, Crawford T, Good E, Oral H, Chugh A, Pelosi F, Morady F, Bogun F. Infarct architecture and characteristics on delayed enhanced magnetic resonance imaging and electroanatomic mapping in patients with postinfarction ventricular arrhythmia. *Heart Rhythm*. 2009;6:644–651.
- Wijnmaalen AP, van der Geest RJ, van Huls van Taxis CF, Siebelink HM, Kroft LJ, Bax JJ, Reiber JH, Schalij MJ, Zeppenfeld K. Head-to-head comparison of contrast-enhanced magnetic resonance imaging and electroanatomical voltage mapping to assess post-infarct scar characteristics in patients with ventricular tachycardias: real-time image integration and reversed registration. *Eur Heart J*. 2011;32:104–114.
- Gerber BL, Belge B, Legros GJ, Lim P, Poncelet A, Pasquet A, Gisellu G, Coche E, Vanoverschelde JL. Characterization of acute and chronic myocardial infarcts by multidetector computed tomography: comparison with contrast-enhanced magnetic resonance. *Circulation*. 2006;113:823–833.
- Kanza RE, Higashino H, Kido T, Kurata A, Saito M, Sugawara Y, Mochizuki T. Quantitative assessment of regional left ventricular wall thickness and thickening using 16 multidetector-row computed tomography: comparison with cine magnetic resonance imaging. *Radiat Med*. 2007;25:119–126.
- Tian J, Jeudy J, Smith MF, Jimenez A, Yin X, Bruce PA, Lei P, Turgeman A, Abbo A, Shekhar R, Saba M, Shorofsky S, Dickfeld T. Three-dimensional contrast-enhanced multidetector CT for anatomic, dynamic, and perfusion characterization of abnormal myocardium to guide ventricular tachycardia ablations. *Circ Arrhythm Electrophysiol*. 2010;3:496–504.
- Stolzmann P, Scheffel H, Leschka S, Schertler T, Frauenfelder T, Kaufmann PA, Marinček B, Alkadhi H. Reference values for quantitative left ventricular and left atrial measurements in cardiac computed tomography. *Eur Radiol*. 2008;18:1625–1634.
- Sosa E, Scanavacca M, d’Avila A, Pilleggi F. A new technique to perform epicardial mapping in the electrophysiology laboratory. *J Cardiovasc Electrophysiol*. 1996;7:531–536.
- West JJ, Patel AR, Kramer CM, Helms AS, Olson ES, Rangavajhala V, Ferguson JD. Dynamic registration of preablation imaging with a catheter geometry to guide ablation in a Swine model: validation of image integration and assessment of catheter navigation accuracy. *J Cardiovasc Electrophysiol*. 2010;21:81–87.
- Gaasch WH, Zile MR. Left ventricular structural remodeling in health and disease: with special emphasis on volume, mass, and geometry. *J Am Coll Cardiol*. 2011;58:1733–1740.
- Saba MM, Akella J, Gammie J, Poston R, Johnson A, Hood RE, Dickfeld TM, Shorofsky SR. The influence of fat thickness on the human epicardial bipolar electrogram characteristics: measurements on patients undergoing open-heart surgery. *Europace*. 2009;11:949–953.
- Arenal A, Glez-Torrecilla E, Ortiz M, Villacastín J, Fdez-Portales J, Sousa E, del Castillo S, Perez de Isla L, Jimenez J, Almendral J. Ablation of electrograms with an isolated, delayed component as treatment of unmappable monomorphic ventricular tachycardias in patients with structural heart disease. *J Am Coll Cardiol*. 2003;41:81–92.
- Bogun F, Good E, Reich S, Elmouchi D, Igic P, Lemola K, Tschopp D, Jongnarangsin K, Oral H, Chugh A, Pelosi F, Morady F. Isolated potentials during sinus rhythm and pace-mapping within scars as guides for ablation of post-infarction ventricular tachycardia. *J Am Coll Cardiol*. 2006;47:2013–2019.
- Brunckhorst CB, Stevenson WG, Jackman WM, Kuck KH, Soejima K, Nakagawa H, Cappato R, Ben-Haim SA. Ventricular mapping during atrial and ventricular pacing. Relationship of multipotential electrograms to ventricular tachycardia reentry circuits after myocardial infarction. *Eur Heart J*. 2002;23:1131–1138.
- Arenal A, del Castillo S, Gonzalez-Torrecilla E, Atienza F, Ortiz M, Jimenez J, Puchol A, García J, Almendral J. Tachycardia-related channel in the scar tissue in patients with sustained monomorphic ventricular tachycardias: influence of the voltage scar definition. *Circulation*. 2004;110:2568–2574.
- Estner HL, Zviman MM, Herzka D, Miller F, Castro V, Nazarian S, Ashikaga H, Dori Y, Berger RD, Calkins H, Lardo AC, Halperin HR. The critical isthmus sites of ischemic ventricular tachycardia are in zones of tissue heterogeneity, visualized by magnetic resonance imaging. *Heart Rhythm*. 2011;8:1942–1949.

22. Verma A, Marrouche NF, Schweikert RA, Saliba W, Wazni O, Cummings J, Abdul-Karim A, Bhargava M, Burkhardt JD, Kilicaslan F, Martin DO, Natale A. Relationship between successful ablation sites and the scar border zone defined by substrate mapping for ventricular tachycardia post-myocardial infarction. *J Cardiovasc Electrophysiol*. 2005;16:465–471.
23. Ciaccio EJ, Ashikaga H, Kaba RA, Cervantes D, Hopenfeld B, Wit AL, Peters NS, McVeigh ER, Garan H, Coromilas J. Model of reentrant ventricular tachycardia based on infarct border zone geometry predicts reentrant circuit features as determined by activation mapping. *Heart Rhythm*. 2007;4:1034–1045.

CLINICAL PERSPECTIVE

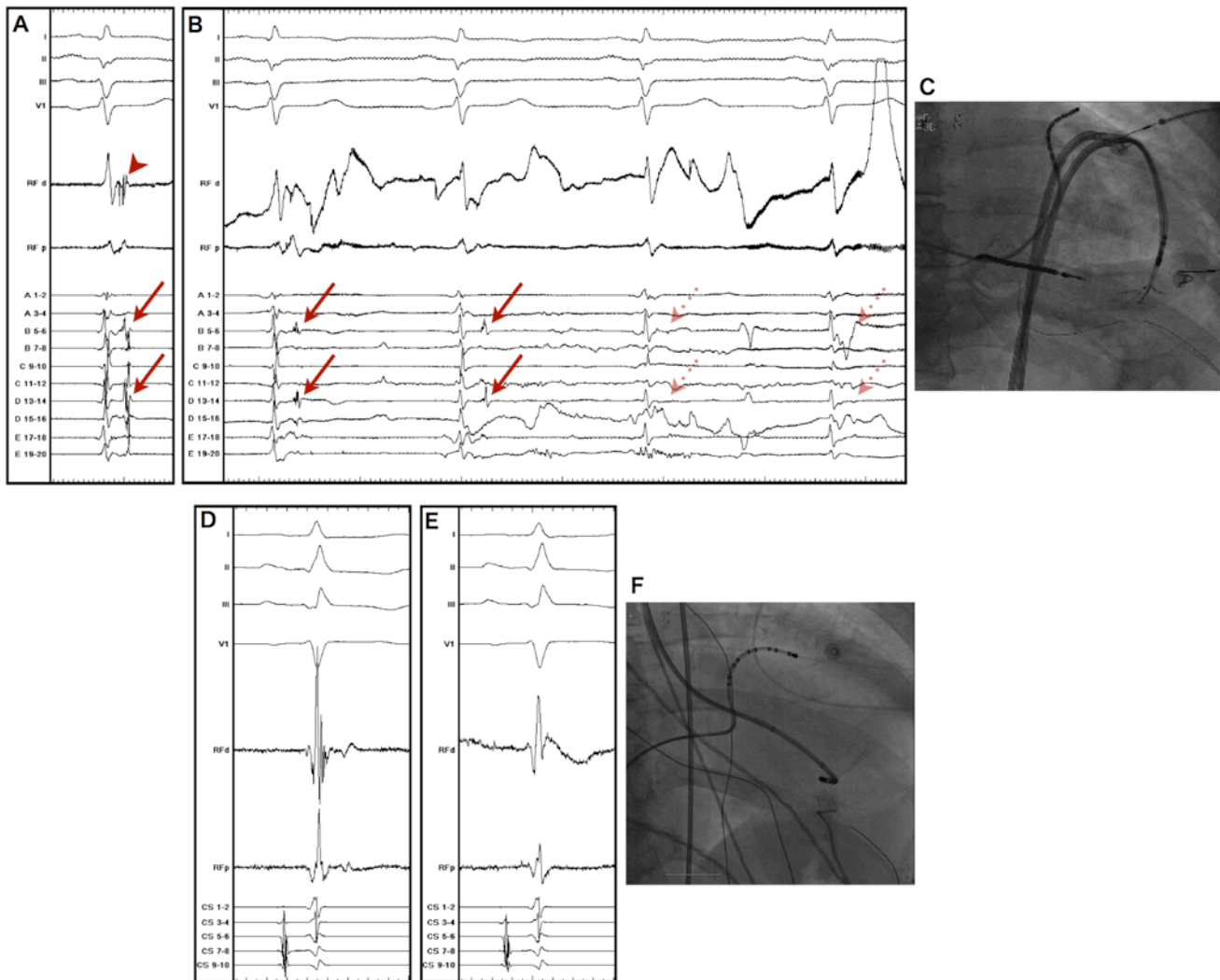
Visualization of ventricular tachycardia substrate obtained by cardiac imaging before and during the procedure can help focus mapping and ablation to the culprit regions. The presence of an implanted cardioverter defibrillator is generally considered to preclude the routine use of MRI in the current standard of care and, in any case, degrades the image quality of anterior aspect of the heart. Contrast-enhanced multidetector computed tomography (MDCT) can depict myocardial wall thickness with submillimetric resolution. We evaluated the relationship between regional myocardial wall thinning (WT) imaged by MDCT and arrhythmogenic substrate in postinfarction ventricular tachycardia. We studied 13 consecutive postinfarction patients undergoing MDCT before ablation. In all patients, MDCT data were successfully integrated with high-density 3D electroanatomic maps acquired during sinus rhythm (endocardium, 509 ± 291 points/map; epicardium, 716 ± 323 points/map). Low-voltage areas (<1.5 mV) and local abnormal ventricular activities (LAVA) during sinus rhythm were assessed with regard to the WT. A significant correlation was found between the areas of WT <5 mm and endocardial low voltage (correlation- $R=0.82$; $P=0.001$), but no such correlation was found in the epicardium. The WT <5 mm area was smaller than the endocardial low-voltage area (54 cm^2 [Q1–Q3, 46–92] versus 71 cm^2 [Q1–Q3, 59–124]; $P=0.001$). Among a total of 13 060 electrograms reviewed in the whole study population, 538 LAVA were detected and analyzed. LAVA were located within the WT <5 mm (469/538 [87%]) or at its border (100% within 23 mm). Very late LAVA (>100 ms after QRS complex) were almost exclusively detected within the thinnest area (93% in the WT <3 mm). In conclusion, regional myocardial WT correlates to low-voltage regions and distribution of LAVA critical for the generation and maintenance of postinfarction ventricular tachycardia. The thinnest areas are associated with the latest electric activities demonstrating a structure–function relationship. The integration of MDCT WT with 3D electroanatomic maps can help focus mapping and ablation on the culprit regions, even when MRI is precluded by the presence of implanted devices.

SUPPLEMENTAL MATERIAL



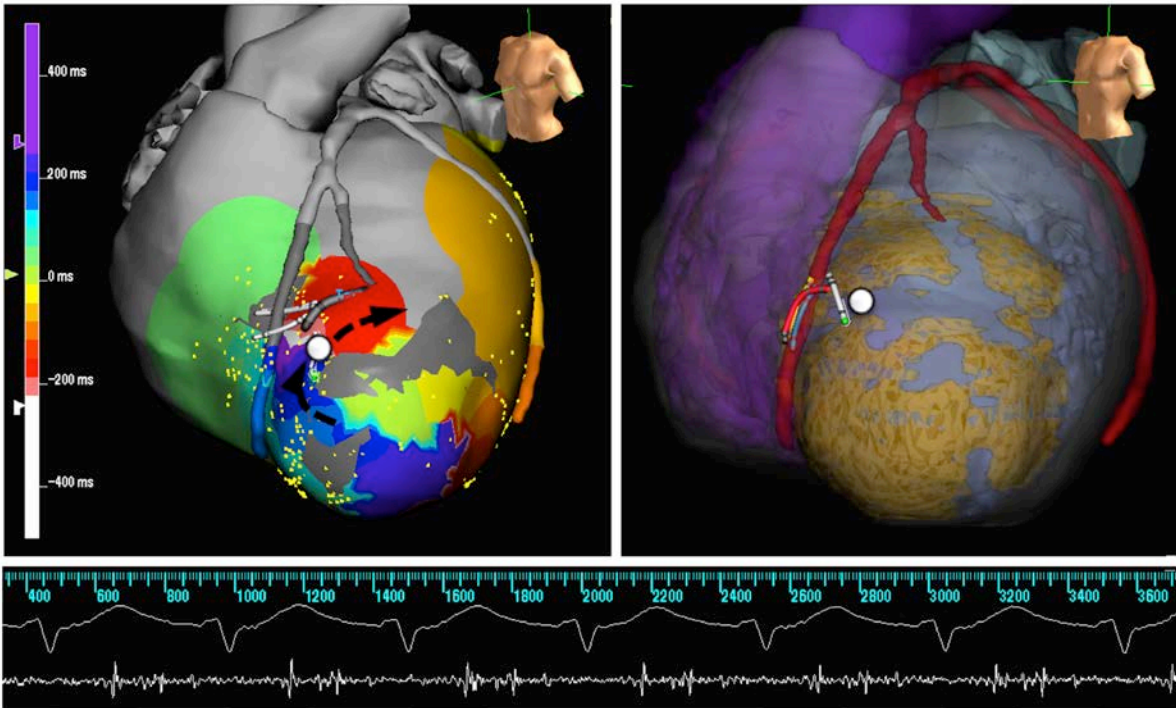
Supplementary Figure 1. Registration methodology.

NavX registration of electroanatomic geometry (**A**) with MDCT-derived model (**B**) demonstrating alignment at multiple corresponding fiducial points. The decapolar catheter, which was placed in the coronary sinus as distally as possible, was carefully registered on the same location in the MDCT model (**C**) and monitored under fluoroscopic guidance (**D**).



Supplementary Figure 2. Ablation of local abnormal ventricular activities (LAVA).

LAVA pre-ablation (A) and during ablation (B) were recorded on the multi-electrode mapping catheter (Pentaray) and ablation catheter placed at the epicardium (C). LAVA recorded on the Pentaray (**arrow**) were later than that on the ablation catheter (**arrow head**). The LAVA recorded on some splines (C9-10 and C11-12) have been already abolished at the 1st beat in (B), and all LAVA were eliminated after the 3rd beat (**dotted arrow**). Another example of the elimination of LAVA is shown in the lower panels (D, E, and F). The non-delayed LAVA which fused with the far-field signal was recorded before ablation (D). After ablation, LAVA was eliminated while the far-field signal remained.



Supplementary Figure 3. The wall thinning (WT) and conducting channel of VT.

The epicardial isochronal map during VT (**upper left**) and the WT<3mm (**upper right**) represent that the location of conducting channel of VT where ablation terminated VT is located in the 3mm<WT<5mm, but flanked by two WT<3mm areas (**white circle tag**). The local electrogram at the success site represents mid-diastolic activity (**lower tracing**).